

First Demonstration of Electron Scattering Using a Novel Target Developed for Short-Lived Nuclei

T. Suda,¹ M. Wakasugi,¹ T. Emoto,¹ K. Ishii,² S. Ito,¹ K. Kurita,² A. Kuwajima,³ A. Noda,⁴ T. Shirai,^{4,*} T. Tamae,³
H. Tongu,⁴ S. Wang,¹ and Y. Yano¹

¹RIKEN Nishina Center, Wako, Saitama 351-0198, Japan

²Department of Physics, Rikkyo University, Toshima, Tokyo 171-8501, Japan

³Laboratory of Nuclear Science, Tohoku University, Sendai, Miyagi 982-0826, Japan

⁴Institute of Chemical Research, Kyoto University, Uji, Kyoto 611-0011, Japan

(Received 10 October 2008; published 13 March 2009)

We carried out a demonstrative electron scattering experiment using a novel ion-trap target exclusively developed for short-lived highly unstable nuclei. Using stable ^{133}Cs ion as a target, this experiment completely mimicked electron scattering off short-lived nuclei. Achieving a luminosity higher than $10^{26} \text{ cm}^{-2} \text{ s}^{-1}$ with around only 10^6 trapped ions on the electron beam, the angular distribution of elastic scattering was successfully measured. This experiment clearly demonstrates that electron scattering off rarely produced short-lived nuclei is practical with this target technique.

DOI: 10.1103/PhysRevLett.102.102501

PACS numbers: 25.30.Bf, 29.20.db, 29.25.Pj

Electron scattering provides the most reliable structure information of atomic nuclei by virtue of the fact that the electron is a pointlike particle, and probes nuclei through the fairly weak and well-understood electromagnetic interaction. The charge density distributions of stable nuclei, which have been precisely determined through measurements of the angular distribution for the elastic scattering cross section [1], have consistently provided a critical testing ground for nuclear structure models.

There are several examples of electron scattering experiments for unstable nuclei having long lifetimes, such as ^3H [2,3] and ^{14}C [4]. However, no experiment with highly unstable (short-lived) nuclei located far from stability has been yet conducted due to the lack of a target forming technique.

Should electron scattering become feasible for short-lived nuclei, the first goal would be to measure the elastic scattering cross section in order to deduce their charge density distributions, as in the case for stable nuclei. While the elastic cross section is largest at low momentum transfer regions, the anticipated low luminosities for experiments involving rarely produced short-lived nuclei might limit the experimentally accessible information of the distribution to gross features such as the radius and surface diffuseness [5]. Despite this limitation, those radial properties along the isotopic chains would be certainly essential to establish nuclear structure models that are applicable for short-lived nuclei. In addition, combined with the matter density distribution obtained by hadron scattering, one can study how the neutron skin develops along the isotopic chain. This study gives an important insight on the equation of state of asymmetric nuclear matter, which plays an essential role in the study of neutron stars [6].

To realize electron scattering experiments for short-lived nuclei, we have proposed a novel internal-target forming technique [7] named SCRIT (self-confining radioactive isotope target), which is based on the well-known “*ion-trapping*” phenomenon that occurs at electron storage rings [8]. A prototype was installed at an electron ring, the KSR (Kaken Storage Ring) [9], at Kyoto University, Japan, to study the practicality of this scheme. We have already reported the success of trapping of externally injected Cs stable ions, and the observation of the scattered electrons at a forward scattering angle of 30° [10]. The electron beam energy was 120 MeV, and the averaged beam current was 75 mA with a lifetime of 100 s. Assuming elastic scattering, the luminosity was estimated to be $2.4 \times 10^{25} \text{ cm}^{-2} \text{ s}^{-1}$.

In this Letter, we report the first demonstration of a real elastic electron scattering experiment with the SCRIT technique. The angular distribution of the scattering cross section in the angular range of 25° – 60° has been successfully measured, which allows unambiguous identification of elastic scattering from the trapped Cs ions.

The prototype, shown in Fig. 1, consists of an external ion source, electrodes for forming the mirror potential to longitudinally localize the trapped Cs ions, an analyzer for monitoring the Cs ions extracted from the trap according to their mass-to-charge ratio, and electron detectors, all of which are in vacuum except the electron detectors.

The scattered electrons emerging to the air through the 1-mm thick Be window are detected by a drift chamber and three calorimeters placed at scattering angles of 30° , 40° , and 60° measured from the trap center.

The drift chamber measures the electron trajectories, from which the scattering angles and the reaction vertices are determined. Each drift cell has a hexagonal shape

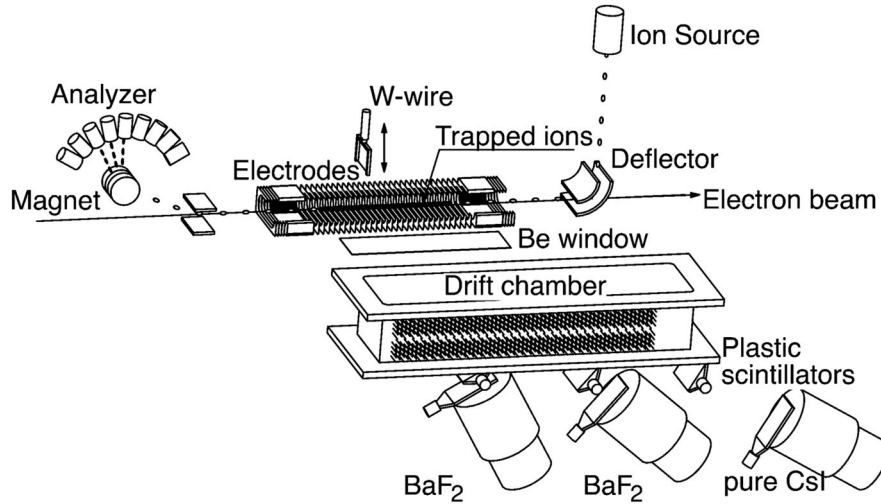


FIG. 1. Setup of the SCRIT prototype consisting of an ion source, a deflector, electrodes for forming the mirror potential, an analyzer, and electron detectors.

enabling a wide range of the scattering angles to be covered. The anode wire sits in the center of the cell, and the maximum drift distance is 18 mm. The drift chamber consists of 128 drift cells which are arranged into two layers. Each of the layers contains two anode wire planes, which are shifted half a pitch with respect to each other in order to eliminate “left-right” ambiguity. The drift chamber was placed so that the distance between the electron beam and the first anode plane was 390 mm. The filling gas was a mixture of helium (50%) and ethane (50%). The electron trajectories are determined by line fitting using the drift time information of fired cells. The space-time relationship is determined using the scattered electrons from the tungsten (*W*) wire inserted very close (~ 1 mm) to the stored electron beam. The vertex resolution obtained by the *W*-wire data is 5 mm, which is well reproduced by a GEANT simulation including the multiple scattering effect which arises in the materials such as the Be window.

For the calorimeters, pure CsI crystals (30°) and BaF_2 crystals (40° and 60°) are employed. Each calorimeter consists of seven optically isolated crystals. The cross section of each crystal is a hexagonal shape having an area of 41.6 cm^2 for CsI and 39.9 cm^2 for BaF_2 . The length of each crystal is 20 cm, corresponding to 10.8 and 9.76 r.l. for CsI and BaF_2 , respectively. The distances from the SCRIT center to the front surfaces of the crystals are 1750 (30°), 1180 (40°), and 790 mm (60°), respectively. The coincidence between a pair of plastic scintillators, $12 \times 12 \text{ cm}^2$ in area, placed in front of each calorimeter defines the solid angle, and triggers data acquisition. The response functions of the calorimeters to 120-MeV electrons are determined by using electrons elastically scattered from the tungsten (*W*) wire. Gain changes of the calorimeters were continuously monitored by a gain monitoring system using an LED.

The injection of the electron beam from the linac to the KSR was repeated every four seconds to maintain a stored beam current of 75 mA on average. We waited for two seconds after the injection to let the electron beam radiatively cool, after which ion-trapping cycles commenced at a frequency of 17 Hz for the following two seconds. The Cs ions were injected every two cycles by controlling the grid of the ion source for repetitive measurements of scattered electrons under conditions with and without the Cs ions. Each ion-trapping cycle began with an extraction of the $250 \mu\text{s}$ -pulsed Cs^{1+} ions at 4.05 kV from the ion source. The Cs ions were merged with the electron beam at the deflector, and guided into the mirror potential. The trap length was set to 260 mm. The potential height of the bottom of the mirror potential was carefully tuned to ensure the kinetic energy of the ions trapped inside the potential was lower than 2 eV.

Precise positioning of the ion beam relative to the stored electron beam was accomplished by using two sets of scrapers installed along the beam path to the electrodes. The absolute position of the electron beam was first determined with an accuracy better than 0.5 mm by using the scrapers, followed by the precise guidance of the ion beam into position.

The trapping time of the ions was set to 50 ms in order to simulate short-lived unstable nuclei. The ions were then released for the measurement of the number of trapped Cs ions and their charge states at the analyzer. From the ion counting by the analyzer, the number of the trapped Cs ions was estimated to be about 2×10^7 at the averaged electron beam current of 75 mA. Note that this number is not necessarily the same as the number of the trapped ions spatially overlapping the electron beam. The spatial overlap between the ions and electron beam was finely tuned and confirmed by observing the increase in the charge state

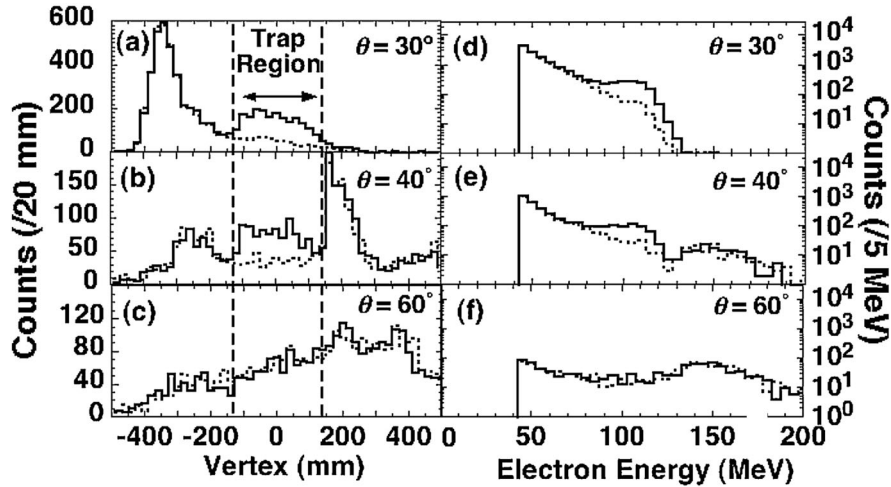


FIG. 2. Electron vertex distributions and energy spectra. Solid (dashed) lines show the distributions measured with (without) trapped Cs ions. (a)–(c) The electron vertex distributions of events detected by the three calorimeters placed at scattering angles of 30°, 40°, and 60°. Events whose energies are larger than 80 MeV are selected. (d)–(f) The energy distributions of the electrons detected by the three calorimeters. Events from the trap region are selected.

of the released Cs ions at the analyzer. The increase is due to further ionization by the stored electron beam through Moeller scattering, which is direct evidence of the spatial overlap between the ions and the electron beam.

Figures 2(a)–2(c) show the vertex distributions of the scattered electron events detected by the three calorimeters, illustrating where scattering takes place. Here, events whose energies are larger than 80 MeV are selected. The net measuring time with Cs ions was 6.5 h. The solid (dashed) line shows the distribution measured with (without) Cs ions. Clear enhancements due to the trapping of the Cs ions are seen in both Figs. 2(a) and 2(b), and the position is consistent with the ion-trapping region set from -130 to 130 mm. The broad peaks outside the trap region seen in Figs. 2(a) and 2(b) are identified due to beam-halo electrons scattered at the thick terminal electrodes. No peak is seen in Fig. 2(a) at the vertex around 200 mm due to the terminal electrodes. This is because there is no acceptance of the electron detector, determined by a pair of plastic scintillators, for this region. A huge electron-loss rate of $\sim 10^8$ s $^{-1}$, which is attributable to the short beam lifetime of the KSR, is the source of the huge beam-halo electrons. No difference due to the trapped Cs ions is observed at these background peaks.

Figures 2(d)–2(f) show the energy spectra of the scattered electrons, whose vertices are in the trapping region. The solid (dashed) lines in the figures are those with (without) the trapped Cs ions. Clear enhancements at around 120 MeV are seen in both Figs. 2(d) and 2(e), whereas they are almost identical in the lower energy region below 80 MeV. Since the spectrum shape of the enhanced events is found to be consistent with the detector response for 120 MeV electrons determined by using the W wire, those events are identified as the elastically

scattered electrons from the trapped Cs. In Fig. 2(f), a slight enhancement for 60° due to the trapped Cs is also seen in the energy region between 80 and 120 MeV. The backgrounds seen in the lower (<80 MeV), and higher (>120 MeV) energy regions are identified to be those from shower-originated electrons (and positrons) due to beam-halo and cosmic rays, respectively.

Using the vertex distributions of the elastic events for 30° and 40° shown in Figs. 2(a) and 2(b), the Cs-ion density distribution along the electron beam is examined. A comparison of the measured vertex distributions with the results of a simulation that takes into account the angular distribution of the elastic scattering cross section and the details of the detector geometry shows that the uniform Cs-ion density distribution along the electron beam reproduces the measured vertex distributions.

Knowing the uniform density distribution of the trapped Cs ions, the distribution of elastic events $N(\theta)$ sorted in accordance with the scattering angle θ is written as

$$N(\theta) = L \frac{d\sigma}{d\Omega} T \int dv \Delta\Omega(\theta, v), \quad (1)$$

where L denotes the luminosity, $d\sigma/d\Omega$ the differential cross section, and T the measuring time. The integral is the effective solid angle of each calorimeter integrated over the vertex coordinate v in the trap region.

Figure 3 shows the angular distribution of the observed elastic events, where the vertical axis denotes $Ld\sigma/d\Omega[(\text{cm}^{-2}\text{s}^{-1})(\text{cm}^2\text{sr}^{-1})]$ calculated according to Eq. (1). Owing to the long trap region of 260 mm, a wide range of scattering angle of 25° to 60° was covered simultaneously using this detector setup. The solid line shows the result of a fit of the data with an elastic cross section for ^{133}Cs calculated using a distorted wave code DREPHA [11],

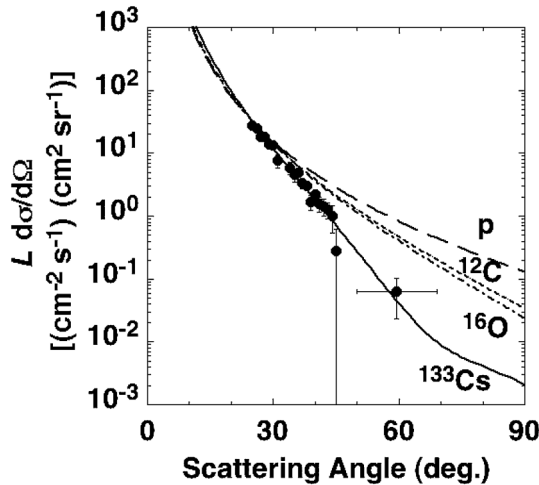


FIG. 3. Angular distribution of electron elastic scattering. Solid circles show the elastic events corrected for geometrical acceptance and measuring time. The solid line shows the results of a fit using the DREPHA results for ^{133}Cs . Dashed, dotted, and dot-dashed lines show the elastic cross section for protons, carbon, and oxygen normalized to the data at a scattering angle of 25° .

where the fitting parameter is the luminosity L . The measured angular dependence over nearly 3 orders of magnitude agrees perfectly with the result of the DREPHA calculation. The parameters for the Cs charge distribution are obtained by scaling the parameters of neighboring nuclei [1], since there is no elastic electron scattering data available for Cs to our knowledge. The associated error in the calculated cross section is estimated to be less than 5%. The radiative correction of about 10% is applied according to Ref. [12].

The dashed, dotted, and dot-dashed lines represent the angular distributions of the elastic scattering cross sections for protons, C and O, which are considered to be the main components of the residual gases in the ring, such as H_2 and CO. The distributions are normalized to the data at a scattering angle of 25° . The angular dependence of the data clearly shows that the detected electrons are those of elastically scattered ones from the trapped ^{133}Cs . While the energy resolution of the calorimeters is not sufficient to resolve elastic scattering from inelastic scattering, the good agreement of the angular dependence with the DWBA calculation may suggest that the contribution of inelastic scattering is still not significant under the current momentum transfer range of 50–120 MeV/ c .

The luminosity achieved is determined to be $1.02(\pm 0.06) \times 10^{26} \text{ cm}^{-2} \text{ s}^{-1}$ by the fit, which is about 4 times higher than the $2.4 \times 10^{25} \text{ cm}^{-2} \text{ s}^{-1}$ obtained in our previous work [10], with the same average electron beam current and a similar number of extracted ions from the ion source. This improvement is attributed to the longer trapping region of 260 mm and the more precise guidance of the ion beam to the electron beam.

Finally, let us estimate the number of the trapped ions on the electron beam. The effective “target thickness,” $N_{\text{ion}} \text{ (cm}^{-2}\text{)}$, can be calculated as $N_{\text{ion}} = L/N_e$, where $L \text{ (cm}^{-2} \text{ s}^{-1}\text{)}$ and $N_e \text{ (s}^{-1}\text{)}$ denote the luminosity and the number of electrons hitting the target every second, respectively. Using $N_e = 4.7 \times 10^{17} \text{ s}^{-1}$ for the averaged beam current of 75 mA, the effective “target thickness” is obtained as $2.2 \times 10^8 \text{ cm}^{-2}$. Considering that the cross section of the electron beam is of the order of 1 mm^2 , the average number of trapped Cs ions located on the electron beam is estimated to be about 10^6 , which is about 1/20 of the number of the trapped ions, 2×10^7 , measured by the analyzer. This efficiency will be improved with a lower-emittance ion beam, which is essential for rarely produced unstable nuclei.

In conclusion, we have succeeded in measuring the angular distribution of elastic scattering using a new ion-trapping technique, SCRIT, with a luminosity of $1.02(\pm 0.06) \times 10^{26} \text{ cm}^{-2} \text{ s}^{-1}$. This was achieved using only 10^6 Cs ions on the electron beam at the average beam current of 75 mA. The measured angular distribution was perfectly reproduced by a distorted wave calculation for ^{133}Cs . This measurement with a trapping time of 50 ms completely mimicked electron scattering off rarely produced short-lived nuclei. The success of the angular distribution of elastic scattering using the new technique with only 10^6 ions is a clear proof that electron scattering off short-lived exotic nuclei is now practical with the SCRIT technology.

This work was supported by Grants-in-Aid for Scientific Research (B) (Grants No. 15340090, No. 15340092, No. 19340073) from JSPS.

*Present address: National Institute of Radiological Sciences, Inage, Chiba 263-8555, Japan.

- [1] H. de Vries, C. W. de Jager, and C. de Vries, *At. Data Nucl. Data Tables* **36**, 495 (1987).
- [2] D. Beck *et al.*, *Phys. Rev. Lett.* **59**, 1537 (1987).
- [3] A. Amroun *et al.*, *Nucl. Phys.* **A579**, 596 (1994).
- [4] F. J. Kline *et al.*, *Nucl. Phys.* **A209**, 381 (1973).
- [5] T. Suda and M. Wakasugi, *Prog. Part. Nucl. Phys.* **55**, 417 (2005).
- [6] K. Oyamatsu *et al.*, *Nucl. Phys.* **A634**, 3 (1998).
- [7] M. Wakasugi, T. Suda, and Y. Yano, *Nucl. Instrum. Methods Phys. Res., Sect. A* **532**, 216 (2004).
- [8] C. J. Bocchetta and A. Wrulich, *Nucl. Instrum. Methods Phys. Res., Sect. A* **278**, 807 (1989).
- [9] A. Noda *et al.*, in *Proceedings of the Fifth European Particle Accelerator Conference, Barcelona*, edited by S. Myers *et al.* (Institute of Physics, Bristol, U.K., 1996), p. 451.
- [10] M. Wakasugi *et al.*, *Phys. Rev. Lett.* **100**, 164801 (2008).
- [11] B. Dreher, DREPHA: a phase-shift calculation code for elastic electron scattering, communicated by J. Friedrich.
- [12] L. W. Mo and T. S. Tsai, *Rev. Mod. Phys.* **41**, 205 (1969).